Acta Pharmacologica Sinica

www.nature.com/aps

ARTICLE

Exosomes are involved in total body irradiation-induced intestinal injury in mice

Hang Li[1], Mian Jiang[1], Shu-ya Zhao[1], Shu-qin Zhang[1], Lu Lu[1], Xin He[1], Guo-xing Feng[1], Xin Wu[1] and Sai-jun Fan[1]

Ionizing radiation-induced intestinal injury is a catastrophic complication in patients receiving radiotherapy. Circulating exosomes from patients undergoing radiotherapy can mediate communication between cells and facilitate a variety of pathological processes in vivo, but its effects on ionizing radiation-induced intestinal damage are undetermined. In this study we investigated the roles of exosomes during total body irradiation (TBI)-induced intestinal injury in vivo and in vitro. We isolated exosomes from serum of donor mice 24 h after lethal dose (9 Gy) TBI (Exo-IR-24h), then intravenously injected the exosomes into receipt mice, and found that Exo-IR-24h injection not only exacerbated 9 Gy TBI-induced lethality and weight loss, but also promoted crypt-villus structural and functional injury of the small intestine in receipt mice. Moreover, Exo-IR-24h injection significantly enhanced the apoptosis and DNA damage of small intestine in receipt mice following TBI exposure. In murine intestinal epithelial MODE-K cells, treatment with Exo-IR-24h significantly promoted 4 Gy ionizing radiation-induced apoptosis, resulting in decreased cell vitality. We further demonstrated that Exo-IR-24h promoted the IR-induced injury in receipt mice partially through its DNA damage-promoting effects and attenuating Nrf2 antioxidant response in irradiated MODE-K cells. In addition, TBI-related miRNAs and their targets in the exosomes of mice were enriched functionally using Gene Ontology (GO) and Kyoto Encyclopedia of Genes and Genomes (KEGG) pathway analyses. Finally, injection of GW4869 (an inhibitor of exosome biogenesis and release, 1.25 mg·kg^{-1}·d^{-1}, ip, for 5 consecutive days starting 3 days before radiation exposure) was able to rescue mice against 9 Gy TBI-induced lethality and intestinal damage. Collectively, this study reveals that exosomes are involved in TBI-induced intestinal injury in mice and provides a new target to protect patients against irradiation-induced intestinal injury during radiotherapy.

Keywords: total body irradiation; radiation-induced intestinal injury; DNA damage; apoptosis; exosome; MicroRNA; GW4869

Acta Pharmacologica Sinica (2021) 42:1111–1123; https://doi.org/10.1038/s41401-021-00615-6

INTRODUCTION

Currently, the increasing threat of nuclear or radiological terrorism, nuclear accidents and the role of radiotherapy in cancer treatment have created the need for radioprotective/mitigating agents that can be useful in radiation protection and therapy [1]. Total body exposure to ionizing radiation (IR) in humans and animals results in multiple organ injury, and IR can damage the gastrointestinal (GI), cerebrovascular, hematopoietic, or central nervous systems depending on the total dose of radiation received [2–5]. One of the most sensitive organs to ionizing radiation in animals is the small intestine [6]. It has been reported that high doses of IR are able to cause intestinal inflammation and associated gut pathologies, induce acute damage to epithelial cells in the intestines and lead to death within 10 days, indicating toxicity to the GI tract [7]. Increasing numbers of promising agents are needed to prevent or remedy IR-induced GI tract toxicity, unlike bone marrow damage, which can be prevented by bone marrow transplantation [8]. Radiation-induced intestinal damage, whose clinical features are anorexia, vomiting, diarrhea, dehydration, systemic infection, septic shock and even death, seriously undermines the efficacy of radiotherapy treatment [9, 10]. Hence, there is an urgent need to identify an effective and safe agent to reduce radiation-induced GI toxicity.

Exosomes, measuring from 30 to 150 nm in diameter, are microvesicles formed in multivesicular bodies, which release the exosomes into the extracellular milieu by fusing with the cell membrane [11, 12]. Exosomes, which are produced by various types of cells, can act as mediators of intercellular communication and affect biological functions by transferring microRNAs (miRNAs), long noncoding RNAs (lncRNAs), proteins, and lipids [13]. Specific proteins, such as Tsg101, CD9, CD63, ALIX, and CD81, are usually used as markers to identify exosomes [14]. Exosomes are also involved in various cellular functions and hence can offer a new tool for diagnostic purposes, such as detecting noninvasive disease or predicting disease progression [15, 16]. In addition, exosomes have been reported to act as new drug delivery vehicles and novel therapeutic tools in various conditions, including cancer, inflammation and regenerative disorders [17, 18].

MicroRNAs (miRNAs) are small, noncoding RNAs that function by inhibiting the translation of target messenger RNAs [19]. It has been reported that exosomes, which contain high levels of miRNAs and exosomal miRNAs, contribute to numerous pathological and

[1]Tianjin Key Laboratory of Radiation Medicine and Molecular Nuclear Medicine, Institute of Radiation Medicine, Chinese Academy of Medical Sciences and Peking Union Medical College, Tianjin 300192, China
Correspondence: Hang Li (lihang@irm-cams.ac.cn) or Sai-jun Fan (fansaijun@irm-cams.ac.cn)

Received: 3 November 2020 Accepted: 15 January 2021
Published online: 26 February 2021

physiological processes and can be a better source of specific miRNAs than whole blood [13, 20]. The increasing interest in miRNAs, a component of exosomal cargo, is due to their stability, as they are contained in exosomes and protected from degradation by RNase in blood [21]. However, the relationship between exosomes (or exosomal miRNAs) and radiation-mediated intestinal injury has not been elucidated.

In this study, we investigated the effects of exosomes during total body irradiation (TBI)-induced intestinal injury in vivo and in vitro. Moreover, due to the various functions of miRNAs in modulating the radiosensitivity of cells, we detected the impact of TBI treatment on the enrichment of miRNAs and their targets in exosomes from mice. The results showed that exosomes are involved in TBI-induced intestinal injury in mice, which is probably mediated by exosomal miRNAs. Our findings provide a new strategy to protect patients against irradiation-induced intestinal injury during radiotherapy.

MATERIALS AND METHODS

Cell culture and treatment

MODE-K murine intestinal epithelial cells were cultured in DMEM (Cat. no. 12400-024, Invitrogen, Carlsbad, CA, USA). Cells were supplemented with heat-inactivated 10% FBS (Cat. no. 10270-106, Gibco, Grand Island, NY, USA), 100 units/mL penicillin (Cat. no. IP0150, Solarbio, Beijing, China), and 100 mg/mL streptomycin (Cat. no. IS0360, Solarbio, Beijing, China) and cultured at 5% CO_2 and 37 °C. Cells were collected and seeded in 6-, 24-, or 96-well plates for 24 h and were then transfected with the corresponding plasmids or siRNAs using Lipofectamine 2000 (Cat. no. 11668-019, Invitrogen, Carlsbad, CA, USA) according to the manufacturer's instructions.

Irradiation studies

A Gammacell® 40 Exactor (Atomic Energy of Canada Limited, Chalk River, ON, Canada) was used for all experiments. For the relevant experiments, mice or cells were exposed to ^{137}Cs γ-ray irradiation (IR) at a dose rate of 0.89 Gy/min before or after treatment with exosomes.

Isolation of exosomes from serum

Different groups of BALB/c mice (as shown in Supplementary Fig. S1a) were sacrificed, and blood was collected in 1.5 mL tubes, incubated at room temperature for half an hour, and centrifuged at 1500 × *g* for 10 min to separate serum. Then, the serum samples were filtered through RNAse/DNAse-free 0.22-μm syringe filters and processed for exosome isolation. A Total Exosome Isolation Kit (Cat. no. UR52136, Umibio, Shanghai, China) was used according to the manufacturers' instructions for exosome isolation from serum samples. Briefly, 100 μL of pretreatment buffer (PB) was added to a GET™ column and centrifuged at 9000 × *g* for 1 min, and 20 μL of equilibrium buffer was then added to the GET™ column and centrifuged at 9000 × *g* for 1 min. Then, cleaned serum/plasma (500 μL of each) was loaded into the GET™ column and centrifuged at 9000 × *g* for 1 min. Ten microliters of release buffer (RB) was then added to the GET™ column, the column membrane was gently rinsed, and the RB was removed. Finally, the GET™ column was transferred to a new collection tube, and 50 μL of collection buffer was added. The membrane was rinsed several times, incubated for 1–2 min, and centrifuged at 9000 × *g* for 3 min; the filtrate was then collected. In brief, 100 μL of exosomes were isolated from 1 mL of mouse serum. The exosomes could be stored at 4 °C for 1 week or −80 °C for 3 months.

Animals and exosome treatment

Six- to eight-week-old male BALB/c mice (average body weight of ~20 g) were purchased from Beijing HFK Bioscience Co., Ltd. (Beijing, China) and housed in the certified animal facility (under specific pathogen-free conditions) at the Institute of Radiation Medicine (IRM) at the Chinese Academy of Medical Sciences (CAMS). The doses and schedules for administration of exosomes and radiation are provided in the relevant figures. In the subsequent experiments, mice were randomized into four groups as follows: (1) control; (2) TBI + vehicle; (3) TBI + Exo-Normal; and (4) TBI + Exo-IR-24h. Mice were subjected to tail vein injection of exosomes at 0.5 mL/kg 2 h after TBI and again 3 days after TBI. All animal experiments were approved by the Institutional Animal Care and Use Committee of the CAMS IRM.

Exosome inhibition

Exosome inhibition was performed using GW4869 (Cat. no. D1692, Sigma, St Louis, MO, USA), a known inhibitor of exosome biogenesis and release. GW4869 was reconstituted in DMSO (Cat. no. D5879, Sigma, St Louis, MO, USA) to a concentration of 5 mM and used as a stock solution for further dilution in 0.1 M PBS (Cat. no. C0221A, Beyotime, Shanghai, China). Mice were injected with 1.25 mg/kg GW4869 via intraperitoneal (ip) injection once daily for 5 days starting 3 days before radiation exposure. A solution of 10% DMSO in 0.1 M PBS was used as the negative control.

Histopathological analysis

Sections (4 μm-thick) of paraffin-embedded small intestinal tissue were dewaxed and rehydrated with citrate buffer and stained with hematoxylin and eosin (H&E), periodic acid-Schiff (PAS), and immunohistochemical (IHC) reagents based on a previous report [22, 23]. For IHC analysis, the sections were boiled in 10 mM citrate buffer solution (pH 9.0) for antigen retrieval according to standard procedures. After antigen retrieval, the sections were incubated first with serum for 1 h at room temperature to block nonspecific antigen-binding sites and then with anti-Lgr5, anti-Ki67, anti-lysozyme or anti-villus antibodies overnight at 4 °C. The sections were then incubated with the secondary antibody for 30 min at 37 °C. Positive-stained cells were detected using a DAB kit (Cat. no. YT9163, Yitabio, Beijing, China). All slides were analyzed, and representative images were acquired using a microscope (Olympus America, Melville, NY, USA).

Crypt microcolony assay

The number of surviving crypts per circumference of transverse intestinal sections was determined from HE-stained sections based on a previous study [24, 25]. Surviving (regenerating) crypts were defined as those containing 10 or more violaceous, thick-walled non-Paneth cells enclosed in a lumen. The number of surviving crypts on each circumference was counted. The fractional crypt survival rate was defined as the ratio (as a percentage) of the number of surviving crypts on the circumference of the intestine in irradiated mice to the number of crypts per cross section in the same region of the intestine in unirradiated (control) mice of the same strain and age.

TUNEL assay

Mice were sacrificed, and their small intestine tissues were harvested and fixed with 4% formaldehyde. The 4 μm-thick sections were treated according to the manufacturer's protocols (Roche, Mannheim, Germany). Briefly, the tissue sections were incubated with a TUNEL reaction mixture for 1 h at 37 °C in the dark. Next, the sections were stained with 0.1 μg/mL DAPI (Cat. no. HY-D0814, MedChemExpress, NJ, USA). FITC-labeled apoptotic cells identified by green fluorescence were observed under an inverted fluorescence microscope (Olympus, Japan).

Immunofluorescence analysis

Paraffin-embedded sections of small intestine tissues were subjected to antigen retrieval as described above and were then washed thoroughly with PBS. The sections were blocked with 5%

goat serum for 30 min at room temperature and were then incubated with anti-γH2AX (Cat. no. 9718, CST, Boston, MA, USA) or anti-p53 (Cat. no. 28961-1-AP, Proteintech, Wuhan, China) antibody overnight at 4 °C. After washing with PBS, the sections were incubated with the secondary antibody for 40 min at 37 °C in the dark. The sections were finally sealed with a DAPI-containing sealing agent. Immunofluorescence staining of cells was performed as described previously [26]. After 48 h of exosome treatment (after 24 h of 4 Gy IR), cells were fixed with paraformaldehyde and permeabilized with 0.1% Triton X-100 (Cat. no. P0096, Beyotime, Shanghai, China) in PBS. After blocking in PBS containing 3% BSA, cells were incubated with primary antibodies at room temperature. After washing with PBS, cells were incubated with a fluorophore-conjugated secondary antibody (Cat. no. BD5002, BioHJ, Xiamen, China) and DAPI. After washing with PBS, slides were mounted with glycerol. Images were acquired by confocal microscopy (Leica TCS SP5, Germany).

Total RNA isolation and real-time PCR

Total RNA was isolated from cells after 2 days of IR using TRIzol reagent (Cat. no. 15596026, Invitrogen, Carlsbad, CA, USA) according to the instructions. First-strand cDNA was synthesized with a PrimeScript Reverse Transcriptase Kit (Cat. no. RR036A, TaKaRa Bio, Dalian, China). For detection of mature microRNAs, total RNA from small intestine tissues of mice was polyadenylated by poly(A) polymerase (Cat. no. ab21867, Abcam, Cambridge, UK) according to the manufacturer's protocol. Reverse transcription was performed using poly(A)-tailed total RNA and reverse transcription primers with ImPro-II Reverse Transcriptase (Cat. no. M5101, Promega, Madison, WI, USA) according to the manufacturer's instructions. Real-time PCR was performed as described previously [27]. The sequences of the primers used in the study are listed in Supplementary Table S1. All experiments were repeated 3 times.

Western blot analysis

For Western blot analysis, total protein was extracted from MODE-K cells with RIPA buffer (Cat. no. R0010, Solarbio, Beijing, China) after 2 days of IR exposure. Proteins were separated by SDS-PAGE and were then transferred to nitrocellulose membranes, which were blocked with 5% nonfat milk and incubated with primary antibodies for 2 h at room temperature. The primary antibodies used were mouse anti-GAPDH (Cat. no. 60004-1-Ig, Proteintech, Wuhan, China), rabbit anti-Nrf2 (Cat. no. 16396-1-AP, Proteintech, Wuhan, China), mouse anti-HO-1 (Cat. no. 27282-1-AP, Proteintech, Wuhan, China), and rabbit anti-NQO1 (Cat. no. 11451-1-AP, Proteintech, Wuhan, China). Then, membranes were incubated with the secondary antibody diluted in PBS at room temperature for 1 h. Membranes were washed in PBS-T, and bound antibody was detected by enhanced chemiluminescence Western Blotting Detection Reagents (Amersham Biosciences, Buckinghamshire, UK). All experiments were repeated 3 times.

CCK-8 assays

MODE-K cells were plated in 6-well plates, cultured for 24 h, and treated with 0, 0.5, 1, 2, 5, or 10 μL of exosomes after exposure to 4 Gy IR. After 24 h of treatment, CCK-8 reagent (Cat. no. E1CK-00208, Enogene, Nanjing, China) was added to the cells for incubation for 1 h. The absorbance at 450 nm was measured in an ELISA plate reader instrument (Labsystems, Multiskan Ascent). All experiments were repeated at least three times.

MTT assays

Cell growth assays were carried out using MTT (3-(4,5-dimethylthiazol-2-yl)-2,5-diphenyltetrazolium bromide) reagent (Cat. no. M2128-1G, Sigma, St Louis, MO, USA) as described previously [28]. In brief, transfected cells were trypsinized, counted, and plated into 6-well plates. After exposure to IR and incubation for different time periods, MTT was added directly to each well and incubated for 4 h. Then, the supernatant was removed, and 100 μL of dimethyl sulfoxide was added to terminate the reaction. The absorbance at 490 nm was measured using the ELISA plate reader instrument (Labsystems, Multiskan Ascent). All experiments were performed in triplicate.

Intracellular ROS assay

MODE-K cells were plated in 6-well plates, cultured for 24 h, and treated with exosomes after exposure to 4 Gy IR. After 24 h of treatment, ROS (reactive oxygen species) levels were determined using a ROS ELISA kit (Cat. no. S0033S, Beyotime, Shanghai, China). In brief, cell culture medium was added to the test sample well. Then, the HRP-conjugated reagent was added to each well, except the blank well. After the plate was sealed with a plate sealing membrane, it was incubated for 60 min at 37 °C. The plate sealing membrane was then removed, the liquid was discarded, washing buffer was added to every well, the plate was incubated for 30 s and was then drained, and the washing procedure was repeated 5 times. Chromogen Solution A and Chromogen Solution B were added to each well, and the plate was incubated in the dark for 15 min at 37 °C. Stop solution was added to each well to terminate the reaction. The absorbance was measured using the ELISA plate reader instrument (Labsystems, Multiskan Ascent) at 450 nm within 15 min after adding the Stop Solution. All experiments were performed in triplicate.

EdU incorporation assay

Cell proliferation was determined after 2 days of IR exposure by a 5-ethynyl-2′-deoxyuridine (EdU) incorporation assay, which was carried out using a Cell-Light^{TM} EdU imaging detection kit (Cat. no. C0078L, Beyotime, Shanghai, China) according to the manufacturer's instructions. All experiments were repeated 3 times.

Statistical analysis

Each experiment was repeated at least three times. Statistical significance was assessed by comparing the mean values (± SDs) using Student's *t* test for independent groups and was assumed for $P < 0.05$ (*), $P < 0.01$ (**) and $P < 0.001$ (***).

RESULTS

Treatment with Exo-IR-24h decreases the survival rate of mice after TBI

To determine the effect of exosomes on mice exposed to radiation, we first collected exosomes from the serum of mice before or after 9 Gy TBI (Supplementary Fig. S1a). Then, a new group of mice was treated with the collected exosomes after exposure to 9 Gy IR (Supplementary Fig. S1b). We found that treatment with Exo-IR-24h decreased the survival rate of mice compared with those of vehicle-treated group and other exosome-treated groups (Supplementary Fig. S1c). Moreover, treatment with Exo-IR-24h significantly exacerbated body weight loss in irradiated mice (Supplementary Fig. S1d) and that the colon length was significantly decreased in Exo-IR-24h-treated mice after exposure to IR (Supplementary Fig. S1e). These results suggested that Exo-IR-24h were probably involved in TBI-induced injury in mice.

In the following study, we further detected the effect of Exo-IR-24h on mice exposed to TBI. The cup-shaped structure, size and number of the isolated exosomes were identified by electron microscopy and NanoSight particle tracking analysis (Fig. 1a, b). In addition, the detection of the characteristic exosome markers Cd63, Tsg101, Cd81, Cd9 and Alix further verified that the isolated particles were exosomes (Fig. 1c). To investigate the relationship between Exo-IR-24h and TBI-induced intestinal damage, irradiated mice in the vehicle- and Exo-Normal-treated groups were selected to compare with irradiated mice in the Exo-IR-24h-treated group.

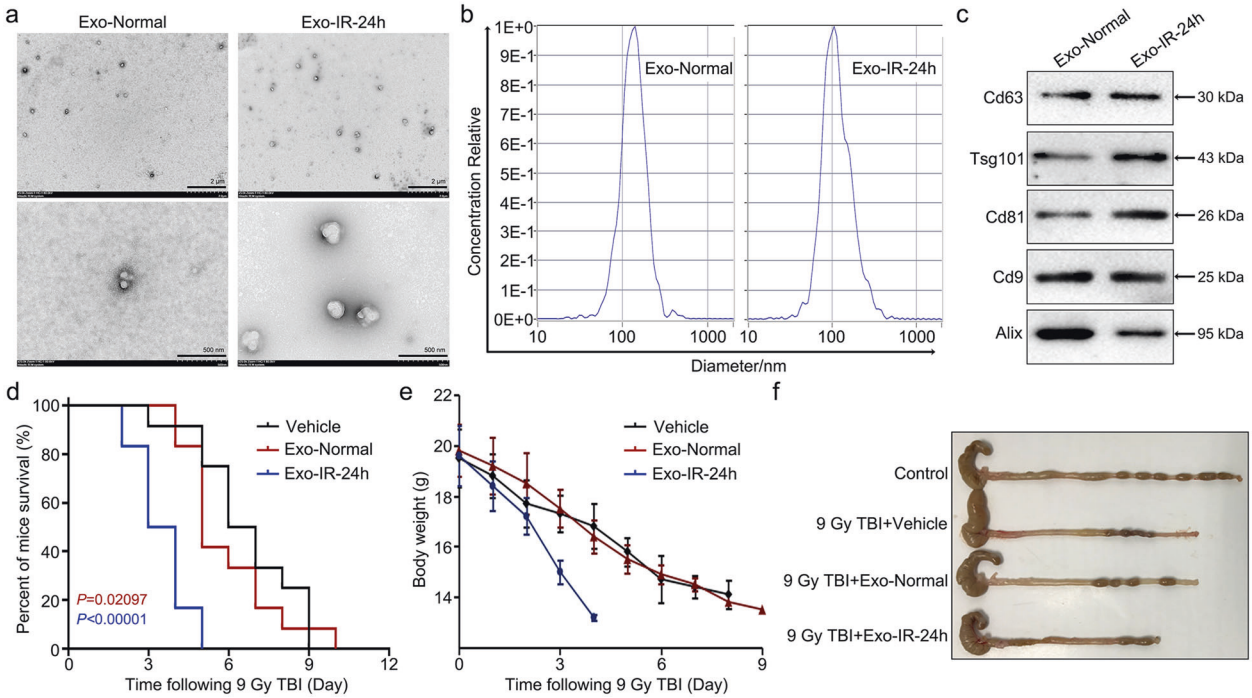

Fig. 1 Exo-IR-24h decreases the survival rate of mice after TBI. a–f Exo-IR-24h, exosomes isolated from the serum of mice after 24 h of TBI; Exo-Normal, exosomes isolated from the serum of mice not exposed to IR. **a** Transmission electron micrograph of exosomes derived from mouse serum. **b** Exosomes released in mice were detected by NanoSight particle tracking analysis. **c** Western blot analysis for detecting the expression of exosomal markers in exosomes. **d** Kaplan–Meier survival analysis of mice after 9 Gy TBI ($n = 12$ mice/group). **e** Body weights of irradiated mice after 9 Gy TBI. **f** Colon tissues from four groups of mice on day 3.5 after 9 Gy TBI are shown.

The results further revealed that Exo-IR-24h exacerbated TBI-induced lethality and weight loss in mice (Fig. 1d, e). In addition, the colon length was reduced by treatment with Exo-IR-24h in mice exposed to IR (Fig. 1f). Thus, the survival rate of mice can be decreased by exosomes secreted in vivo after 24 h of TBI.

Treatment with Exo-IR-24h enhances TBI-induced small intestinal damage in mice

To further validate the role of exosomes in radiation-induced intestinal injury in mice, we examined the morphological changes in mouse small intestines at 3.5 days after 9 Gy TBI with or without exosome treatment (Fig. 2a). Our results showed that the contents of the small intestine were reduced and watery diarrhea appeared in mice exposed to IR. However, the symptoms caused by TBI were exacerbated in mice treated with Exo-IR-24h (Fig. 2b). Next, H&E staining revealed that irradiated mice showed significantly shorter villus lengths and fewer surviving crypts than mice in the control group, and this phenomenon was enhanced by treatment with Exo-IR-24h (Fig. 2c and Supplementary Fig. S2). These results suggested that TBI-induced small intestinal damage was exacerbated by Exo-IR-24h in mice.

Goblet cells play a critical role in barrier function since these particular intestinal epithelial cells not only produce mucins but also secrete factors regulating epithelial renewal and healing [29]. PAS staining analysis showed that the number of goblet cells was markedly decreased in mice at 3.5 days after TBI; however, administration of Exo-IR-24h further reduced the number of goblet cells in the small intestine (Fig. 2d, e). Collectively, these results indicated that Exo-IR-24h enhanced TBI-induced small intestinal damage in mice.

Treatment with Exo-IR-24h attenuates ISC survival and abolishes the regeneration of intestinal cells after TBI

In the gut epithelium, intestinal stem cells (ISCs) expressing leucine-rich repeat-containing G protein-coupled receptor 5 (Lgr5) are located at the bottom of crypts and are actively cycling [30]. $Lgr5^+$ ISCs constantly self-renew at the base of intestinal crypts throughout the organism's life and are indispensable for intestinal regeneration after radiation exposure [31, 32]. To evaluate the effect of exosomes on the proliferation and differentiation abilities of crypt cells, we performed IHC staining to detect $Lgr5^+$ and $Ki67^+$ cells. Our results revealed that the number of Lgr5-expressing cells was significantly decreased in Exo-IR-24h-treated mice compared with mice in other groups after TBI (Fig. 3a and Supplementary Fig. S3a). Similarly, the number of Ki67-positive cells in Exo-IR-24h-treated mice was also markedly lower than that in mice in the TBI groups (Fig. 3b and Supplementary Fig. S3b), suggesting that the proliferation and differentiation abilities of intestinal cells can be damaged by Exo-IR-24h in mice. Paneth cells, one lineage of small intestinal epithelial cells, secrete the antimicrobial peptide α-defensin and contribute to enteric innate immunity through their microbicidal activities [33]. Villin is an actin-binding cytoskeletal protein that associates with the apex and axial bundle structures of intestinal microvilli and is responsible for cytoskeletal organization in the intestine [34]. Hence, we detected the levels of $lysozyme^+$ Paneth cells and $villin^+$ enterocytes to further validate the effect of exosomes on the regeneration of intestinal cells in irradiated mice. As expected, the numbers of $lysozyme^+$ Paneth cells and $villin^+$ cells were significantly decreased in the TBI cohorts compared with the control group, and injury was exacerbated by treatment with Exo-IR-24h (Fig. 3c, d and Supplementary Fig. S3c, d). Thus, our results demonstrated that Exo-IR-24h attenuated ISC survival and abolished the regeneration of intestinal cells after TBI.

Treatment with Exo-IR-24h promotes apoptosis and DNA damage in the small intestine in mice exposed to TBI

To investigate the role of exosomes in small intestinal apoptosis after TBI, we performed terminal deoxynucleotidyl transferase (dUTP) nick end labeling (TUNEL) assays to analyze the apoptosis

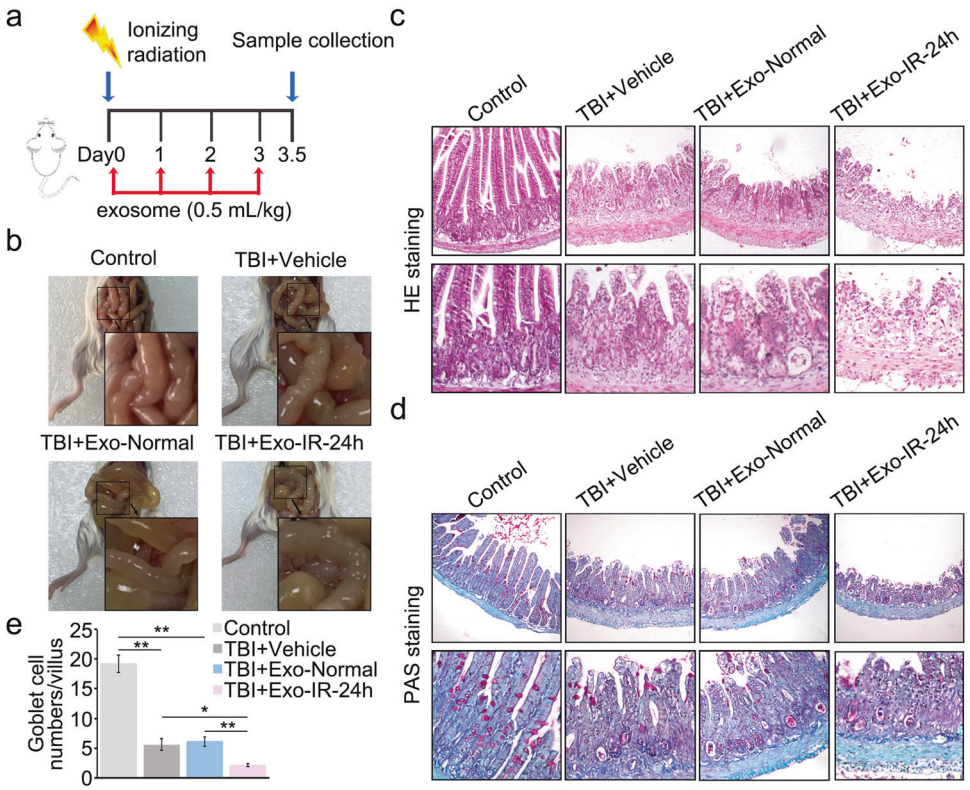

Fig. 2 Exo-IR-24h enhances TBI-induced small intestinal damage in mice. a Mice received intravenous administration of vehicle (5% DMSO)/exosomes 2 h after TBI and then 3 days following TBI. Mice were sacrificed, and small intestine segments were collected on day 3.5, as illustrated in the diagram ($n = 6$ mice/group). **b** Representative images of the respective intestinal tracts. **c** Representative images showing the structure in small intestine cross sections stained with hematoxylin and eosin (H&E). Magnification: ×200 (top), ×400 (bottom). **d** Representative images of periodic acid-Schiff (PAS) staining. Magnification: ×200 (top), ×400 (bottom). **e** Quantification of goblet cells based on PAS staining. The data are representative of three independent experiments; Student's *t* test; $^{*}P < 0.05$; $^{**}P < 0.01$.

of small intestinal tissues in mice. We found that there were a large number of apoptotic cells in the crypts and villi in irradiated mice compared with control mice and that treatment with Exo-IR-24h significantly increased the apoptosis level in the small intestine in mice (Fig. 4a, d). Moreover, immunofluorescence analysis was performed to evaluate the expression level of the p53 protein in intestinal tissues. The results showed that the expression of p53 in irradiated mice was higher than that in control mice and that this increase was enhanced by treatment with Exo-IR-24h (Fig. 4b, e). These data indicated that the apoptosis of small intestinal tissues in TBI-treated mice was increased by treatment with Exo-IR-24h. The most severe type of DNA damage caused by ionizing radiation is the double-strand break (DSB), which is followed by phosphorylation of the second histone (H2A) protein on serine 139, converting it to γH2AX, in nucleosomes [35]. Hence, we evaluated DSBs by performing immunofluorescence staining to analyze the phosphorylation of histone H2AX in order to determine the effect of exosomes on DNA damage in the small intestines of irradiated mice. There was an increase in γH2AX expression in intestinal sections from irradiated mice compared with control mice, and the damage was exacerbated by treatment with Exo-IR-24h (Fig. 4c, f). Collectively, these results indicated that Exo-IR-24h promoted apoptosis and DNA damage in the small intestines of mice exposed to TBI.

Treatment with Exo-IR-24h suppresses cell proliferation and enhances oxidative DNA damage in irradiated MODE-K cells

Next, we used MODE-K murine intestinal epithelial cells to investigate the effect of exosomes during IR-induced GI tract syndromes in vitro. First, the doses of Exo-IR-24h effective at modifying the growth of irradiated MODE-K cells were determined through CCK-8 assays (Fig. 5a). Exposure to IR induced a significant reduction in cell viability compared to that in the control group, and treatment with Exo-Normal had no effect on the IR-mediated suppression of cell growth (Fig. 5b). However, the IR-induced decrease in cell viability was enhanced by treatment with Exo-IR-24h (Fig. 5b). Moreover, the results of the EdU and MTT assays demonstrated that exposure to IR was able to suppress the proliferation of MODE-K cells and that this suppression was enhanced by treatment with Exo-IR-24h (Fig. 5c, d). These results suggested that Exo-IR-24h suppressed the proliferation of irradiated cells. IR-induced DNA and protein damage are mainly mediated by elevated reactive oxidative species (ROS) levels, and ROS can destroy unsaturated fatty acids to decrease the activity of enzymes related to antioxidation [36]. Our results showed a significant increase in intracellular ROS levels after IR exposure, and treatment with Exo-IR-24h further increased ROS production in irradiated MODE-K cells (Fig. 5e). 8-Hydroxy-2′-deoxyguanosine (8-OHdG) is a reporter of oxidative damage to DNA [37, 38]. Immunofluorescence analysis was performed, and the results revealed that the number of H2AX foci and the expression of 8-OHdG were significantly higher in IR-treated MODE-K cells than in control cells and that the damage was enhanced by treatment with Exo-IR-24h (Fig. 5f–h). Thus, we concluded that treatment with Exo-IR-24h suppressed cell proliferation and enhanced ROS-regulated oxidative DNA damage in irradiated MODE-K cells.

Treatment with Exo-IR-24h promotes IR-induced DNA damage and apoptosis by attenuating the Nrf2-mediated antioxidant response in MODE-K cells

Nuclear factor erythroid-2 related factor 2 (Nrf2) is a basic leucine zipper transcription factor that regulates a coordinated transcriptional

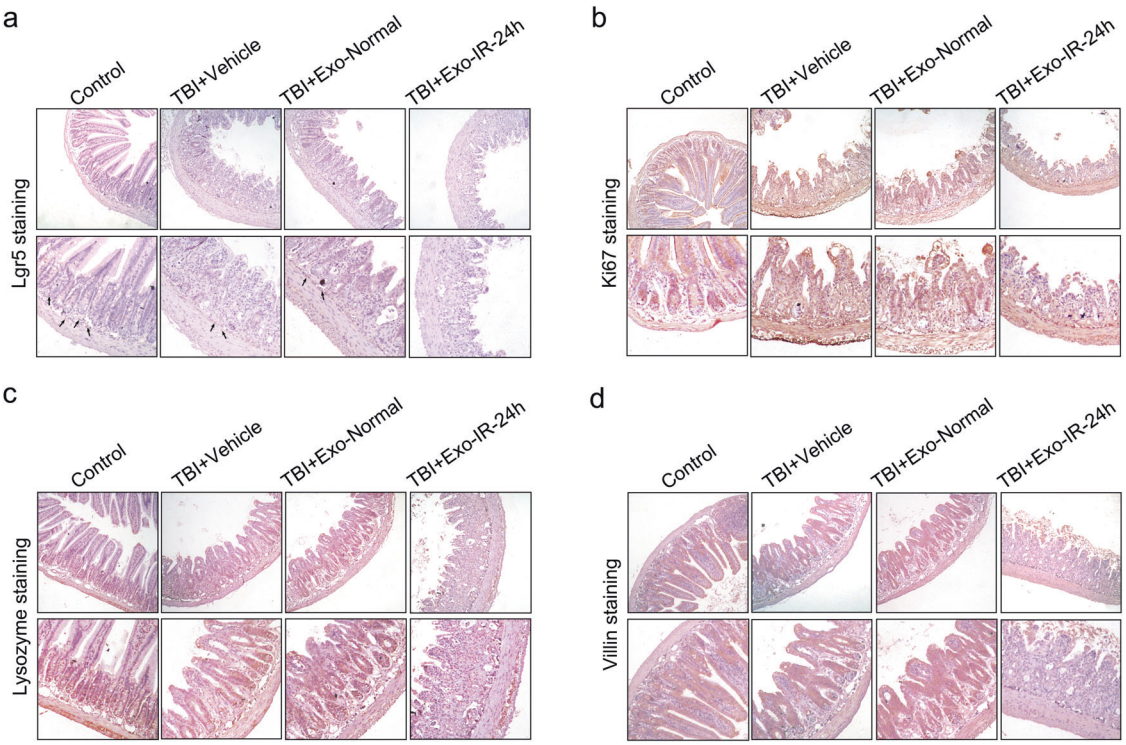

Fig. 3 Exo-IR-24h attenuates ISC survival and abolishes the regeneration of intestinal cells after TBI. Mice were sham-irradiated or subjected to 9 Gy TBI after receiving injections of vehicle or exosomes, as illustrated in the diagram. Representative images of the expression of $Lgr5^+$ (**a**), $Ki67^+$ (**b**), $lysozyme^+$ (**c**) and $villin^+$ (**d**) in small intestine cross sections as shown by immunohistochemical (IHC) staining on day 3.5 after irradiation. Magnification: ×200 (top), ×400 (bottom).

program to scavenge reactive oxygen species and protect cells against DNA damage and apoptosis after irradiation [39, 40]. Hence, we detected the mRNA levels of Nrf2 in MODE-K cells through real-time PCR analysis. The results revealed that IR exposure increased the expression levels of Nrf2, whereas this upregulation was abolished by treatment with Exo-IR-24h (Fig. 6a). Furthermore, we performed Western blot analysis to determine the protein levels of Nrf2 in MODE-K cells and found that the IR-induced increase in the expression level of Nrf2 was reduced by treatment with Exo-IR-24h (Fig. 6b, c). These data suggested that Exo-IR-24h decreased the expression of Nrf2 at the mRNA and protein levels in MODE-K cells after radiation exposure. In addition, the results of the real-time PCR and Western blot analyses demonstrated that the expression levels of the antioxidant proteins HO-1 and NQO1, which are downstream targets of the Nrf2 pathway and are upregulated by IR, were suppressed by treatment with Exo-IR-24h in MODE-K cells (Fig. 6a–e), indicating that Nrf2 signaling was inactivated by treatment with Exo-IR-24h in these cells. Collectively, these results indicated that treatment with Exo-IR-24h promoted IR-induced DNA damage and apoptosis by attenuating the Nrf2-mediated antioxidant response in MODE-K cells.

Total body irradiation modulates the expression level of exosomal miRNAs in mice

Exosomes act as intercellular shuttles to deliver important messages to alter the gene expression and cellular functions of distant organs through proteins, lipids, DNA, long noncoding RNAs (lncRNAs) and, especially, functional miRNAs [41]. Accordingly, we identified small RNAs (sRNAs) in mouse exosomes before or after TBI by deep sequencing. The results demonstrated that the sRNA contents were altered by TBI and that miRNAs had the highest abundance among the sRNAs in mouse exosomes (Fig. 7a, b, Supplementary Tables S2 and S3). Then, the distributions of the first nucleotides of the miRNAs in mouse exosomes were analyzed by deep sequencing (Fig. 7c). Moreover, a total of 1080 TBI-upregulated and 396 TBI-downregulated miRNAs in mouse exosomes were identified based on fold changes in expression (≥ 1 or ≤ -1), as indicated by the histogram and volcano plot (Fig. 7d, e, Supplementary Table S4). Finally, the differential expression of 1856 miRNAs between exosomes from mice with or without TBI was shown on a heatmap (Fig. 7f, left; Supplementary Table S5). Among these miRNAs, 200 differentially expressed miRNAs were identified based on the P value ($P < 0.05$) (Fig. 7f, right; Supplementary Table S6). Thus, these results demonstrate that TBI can remodel the contents of exosomes and modulate the expression of miRNAs in mouse exosomes.

Total body irradiation induces intestinal injury through serum exosomal miRNAs in mice

To investigate the mechanism by which exosome-mediated intestinal damage is induced by TBI, we performed GO and KEGG analyses to elucidate the biological functions of the target genes of serum exosomal miRNAs from mice (Supplementary Table S7). We found that many of the enriched GO biological process (BP) terms were related to the regulation of cell killing, cell growth and cell signaling (Fig. 8a). Then, KEGG enrichment analysis demonstrated that many of the target genes participated in oxidative phosphorylation, nucleotide excision repair and the cell cycle (Fig. 8b). Furthermore, the secondary significantly enriched KEGG pathways were those related to cell growth and death, DNA replication and repair, and energy metabolism (Fig. 8c). These results reveal that exosomal miRNAs can mediate TBI-induced intestinal damage in mice.

Next, heatmap analysis was performed with the miRNAs involved in radiation damage signaling to further characterize the relationship between exosomes and TBI-induced intestinal injury. A total of 468 apoptosis- and DNA damage-related miRNAs were revealed to be differentially expressed between exosomes

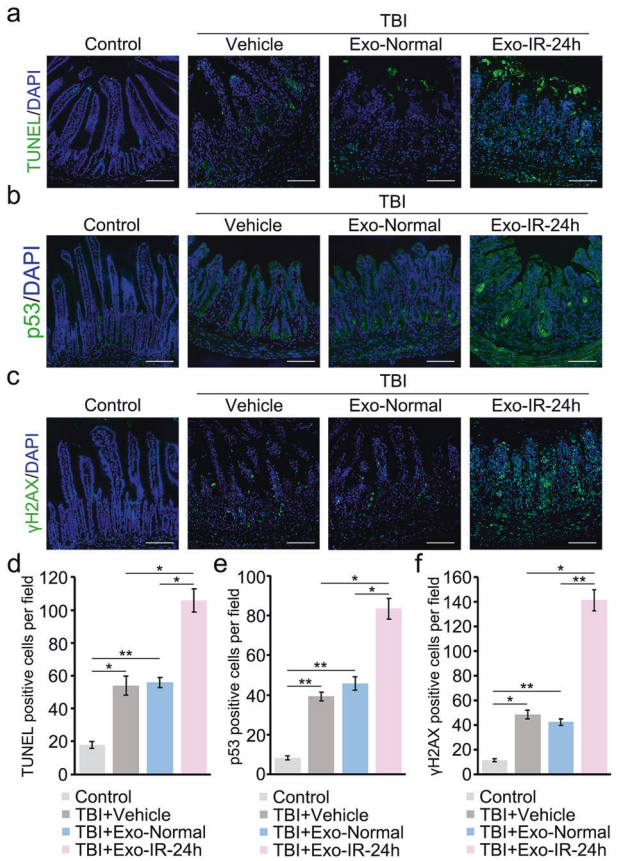

Fig. 4 Exo-IR-24h promotes apoptosis and DNA damage in the small intestines of mice exposed to TBI. a Apoptosis in the small intestine was evaluated by a TUNEL assay. Scale bar: 100 μm. **b** Representative immunofluorescence images showing the expression of p53 in the small intestine (green, p53; blue, DAPI). Scale bar: 100 μm. **c** Representative immunofluorescence images showing the expression of γH2AX in the small intestine (green, γH2AX; blue, DAPI). Scale bar: 100 μm. The numbers of TUNEL-positive cells (**d**), p53-positive cells (**e**), and γH2AX-positive cells (**f**) per field of view were determined. The data are representative of three independent experiments; Student's *t* test; $^{*}P < 0.05$; $^{**}P < 0.01$.

from mice with or without TBI (Fig. 9a, Supplementary Table S8). In addition, a total of 715 proliferation- and cell growth-related miRNAs were differentially expressed between exosomes of mice with or without exposure to IR (Fig. 9b, Supplementary Table S9). Moreover, the expression levels of 5 miRNAs (randomly selected from those listed in Supplementary Tables S8 and S9) in the intestinal tissues of mice treated with Exo-Normal or Exo-IR-24h after TBI were determined using real-time PCR. Our findings showed that the exosomal miRNAs modulated by TBI were also expressed in the intestines of mice (Fig. 9c–g), supporting our finding that the exosomal miRNAs were involved in TBI-induced intestinal injury. GW4869, a neutral sphingomyelinase 2 (nSMase2) inhibitor, is a widely used blocker of exosome secretion that acts by reducing ceramide-dependent exosome production [42]. Then, we observed that treatment with GW4869 improved the survival rate and reduced body weight loss in mice exposed to TBI (Fig. 9h, Supplementary Fig. S4a). Moreover, the colon length in mice exposed to IR was increased by GW4869 treatment (Supplementary Fig. S4b). In addition, treatment with GW4869 attenuated small intestine damage and restored crypt survival and villus length in mice after TBI (Supplementary Fig. S4c–f). These results suggested that inhibition of exosome biogenesis after 24 h of TBI protected mice against TBI-induced lethality and ameliorated IR-induced intestinal injury. In conclusion, TBI induces intestinal injury in mice through miRNAs contained in exosomes secreted in vivo after 24 h of TBI.

DISCUSSION

The GI system is a major target for somatic injury resulting from cancer therapy, nuclear accidents, and radiological terrorism [43]. Gastrointestinal toxicity is reported to be initiated by exposure to high doses of radiation (>8 Gy), and it then contributes to lethality in the absence of intervention [1]. Many studies have reported that bone marrow transplantation or growth factor administration can be used to treat radiation victims with hematopoietic injury and thus reduce TBI-induced injury [44, 45], but there are no suitable interventions available for human use to prevent radiation-induced GI damage. Hence, it is important to illustrate the mechanism of radiation-induced intestinal injury and develop strategies or drugs to mitigate TBI-induced injury. Numerous research reports have pointed out that exosomes not only function in removing cellular artifacts but also play an important role in cell-to-cell communication and many biological processes [21]. However, little is known about the correlation between exosomes and TBI-induced intestinal injury. Herein, we first revealed that exosomes containing exosomal miRNAs are involved in TBI-induced intestinal injury in mice.

In this study, we speculated that exosomes secreted by cells in vivo might play an important role in TBI-induced GI damage in mice. To validate this hypothesis, we thoroughly determined the functions of exosomes during radiation-induced injury in this research. We first isolated exosomes from the serum of mice before or after 9 Gy TBI, and we determined whether these exosomes could aggravate or ameliorate IR-induced intestinal injury in a mouse model of TBI. Interestingly, the results indicated that exosomes isolated from the serum of mice after 24 h of TBI (Exo-IR-24h) decreased the overall survival rate of mice after 9 Gy TBI, while other groups of exosomes had no significant effect on mice exposed to radiation. This finding suggested that Exo-IR-24h were probably involved in TBI-induced intestinal injury in mice, and this conclusion was confirmed in our further investigations. According to previous research, goblet cells produce mucins and secrete factors regulating epithelial renewal; hence, among intestinal epithelial cells, goblet cells play a critical role in barrier function [46]. Our results showed that treatment with Exo-IR-24h reduced the number of goblet cells in the small intestine to enhance TBI-induced small intestinal damage in mice. Total body irradiation causes various degrees of villus blunting and fusion and induces severe loss of crypts, resulting in destruction of epithelial integrity [47]. The intestinal epithelium is one of the most rapidly self-renewing tissues in animals and can be renewed by ISCs located in crypts [48]. Therefore, ISCs, which are characterized by Lgr5 expression, are necessary to maintain homeostasis and crucial for regeneration of the intestinal structure [49]. In addition, epithelial homeostasis is maintained by proliferative cells in crypts, and small intestinal crypt cells are particularly sensitive to IR due to their high proliferation rate [50]. We found that treatment with Exo-IR-24h reduced $Lgr5^{+}$ cell levels and further abolished the regenerative capacity of intestinal cells, decreasing the numbers of $lysozyme^{+}$ Paneth cells, $villin^{+}$ cells and $Ki67^{+}$ instantaneously amplifying cells in irradiated mice. Hence, our results preliminarily reveal that treatment with Exo-IR-24h exacerbates IR-induced injury to the small intestine and further attenuates the regenerative capacity of the intestinal epithelium in mice after TBI.

Apoptosis is a mechanism that removes unwanted cells in tissues and involves the controlled breakdown of intracellular

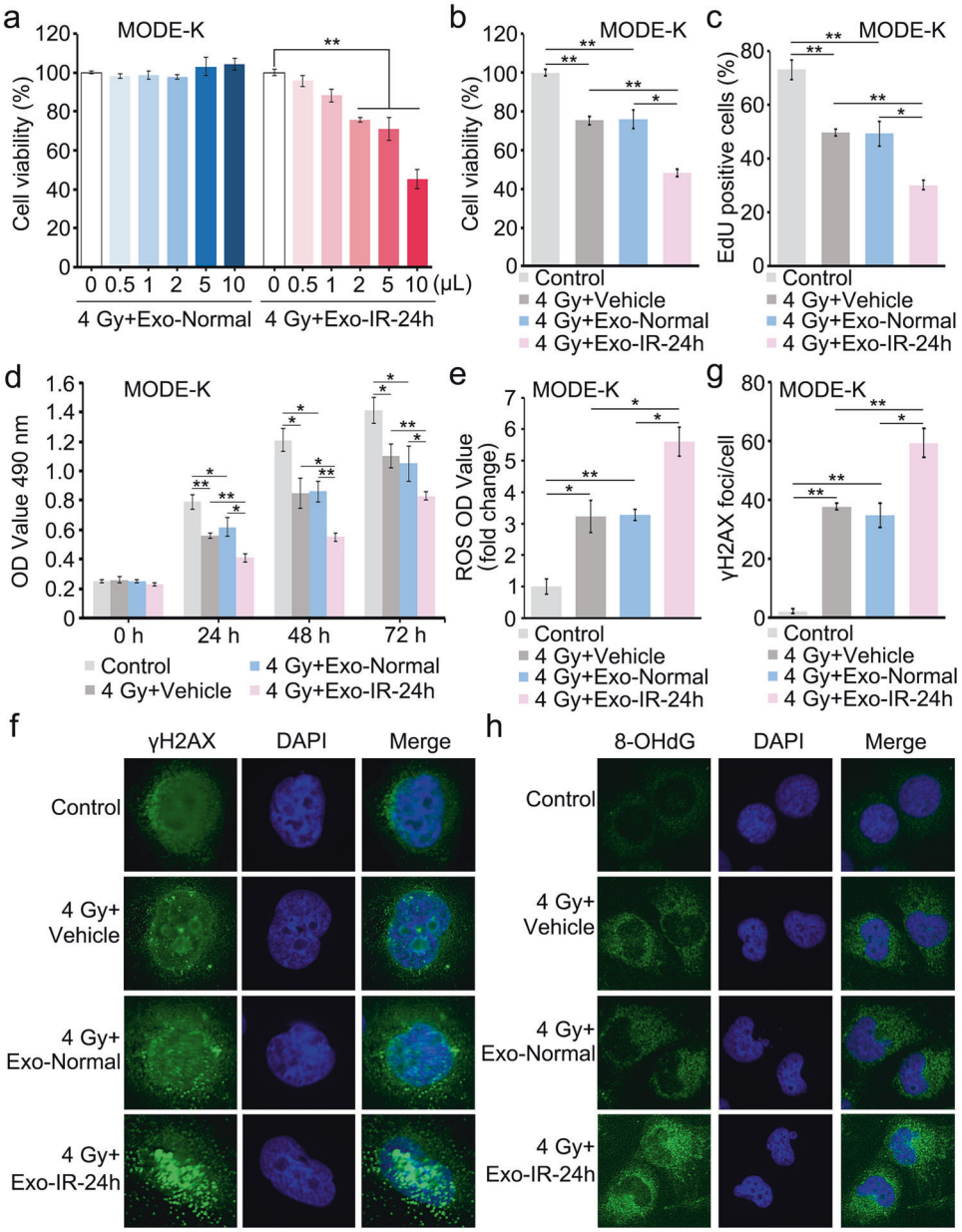

Fig. 5 Exo-IR-24h suppresses cell proliferation and enhances oxidative DNA damage in irradiated MODE-K cells. a Effective doses of exosomes in MODE-K cells were identified using a CCK-8 assay. Then, a dose of 5 μL of exosomes/well (6-well plates) was used in the following experiments. **b** The viability of MODE-K cells was evaluated by a CCK-8 assay. **c** The growth of MODE-K cells was assessed by an EdU incorporation assay. **d** The proliferation of MODE-K cells was validated by a MTT assay. **e** The levels of intracellular reactive oxygen species (ROS) in MODE-K cells were determined by ELISA. **f** The formation of γH2AX foci was evaluated by immunofluorescence in MODE-K cells (×400 magnification). **g** The numbers of γH2AX foci (green) per cell were determined. **h** The expression of 8-hydroxy-2′-deoxyguanosine (8-OHdG) was measured by immunofluorescence (×400 magnification). The data are representative of three independent experiments; Student's *t* test; **P* < 0.05; ***P* < 0.01.

components [51]. It has been reported that IR can induce damage to small intestine tissues and increase the level of intestinal cell apoptosis [52, 53]. Many studies have revealed that p53 is a multifunctional protein that determines cell fate in response to cellular stress [54]. p53 can be activated under severe stress and induce cell cycle arrest, DNA repair, senescence, or apoptosis, depending on the specific transcriptional targets (i.e., *p21*, *BcL2*, *Sesn1*, and *Sesn2*) that are activated [55]. In this study, we found that treatment with Exo-IR-24h further promoted the IR-induced increase in apoptosis and elevation in the p53 level in intestinal tissues. Histone H2AX is one of several variants of nucleosome core histone H2A family proteins, and phosphorylation of H2AX can be induced by DNA damage caused by ionizing radiation [56, 57]. Therefore, phosphorylation of histone H2AX on Ser-139 (γH2AX) is a common indicator used to quantify DNA damage, particularly when the damage involves the presence of DNA double-strand breaks (DSBs) [58]. Our results demonstrated that treatment with Exo-IR-24h enhanced the increase in histone H2AX phosphorylation in the small intestines of mice normally observed after TBI. These data suggest that IR induces apoptosis and DNA damage in the intestine, probably through exosomes secreted in mice 24 h after TBI.

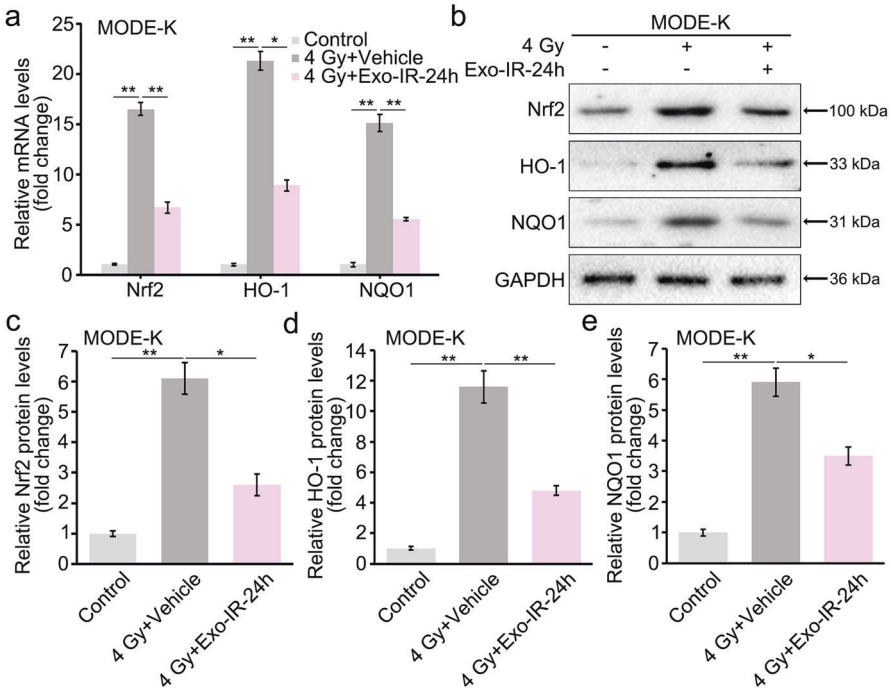

Fig. 6 Exo-IR-24h promotes IR-induced DNA damage and apoptosis by attenuating the Nrf2-mediated antioxidant response in MODE-K cells. a The expression levels of Nrf2, HO-1, and NOQ1 in MODE-K cells were determined by real-time PCR. **b** Western blot analysis of Nrf2, HO-1, and NOQ1 in MODE-K cells. **c**–**e** Relative quantification of Nrf2, HO-1, and NOQ1 protein levels in MODE-K cells. The data are representative of three independent experiments; Student's *t* test; $^{*}P < 0.05$; $^{**}P < 0.01$.

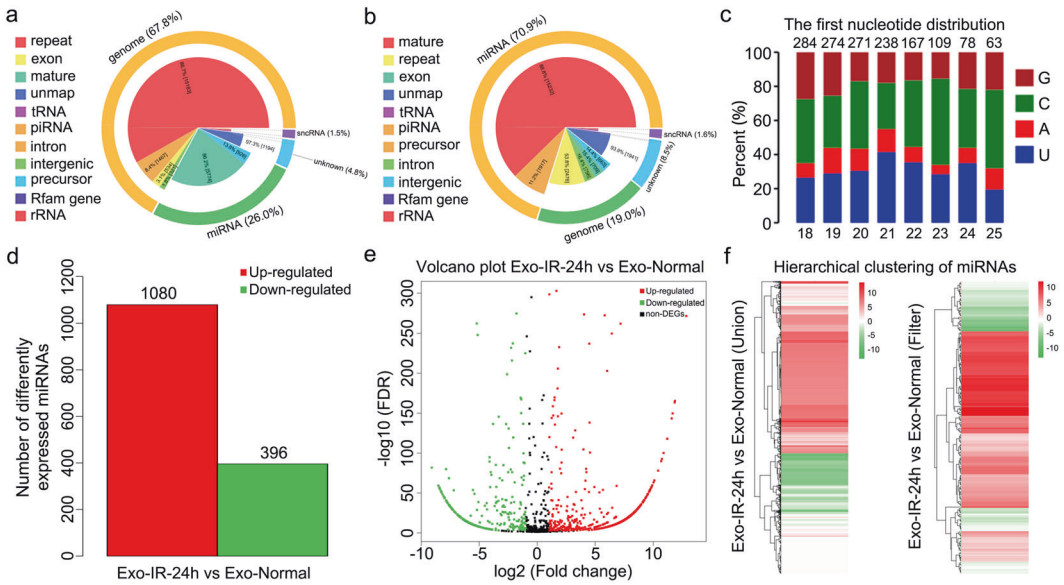

Fig. 7 Total body irradiation modulates the expression levels of exosomal miRNAs in mice. a sRNA contents in Exo-Normal. **b** sRNA contents in Exo-IR-24h. **c** The distributions of the first nucleotides in exosomal miRNAs were analyzed by deep sequencing. **d**, **e** The TBI-modulated miRNAs in the exosomes of mice were identified based on fold changes in expression (≥1 or≤−1), as shown by the histogram (**d**) and volcano plot (**e**). **f** Differential expression of the miRNAs between Exo-Normal and Exo-IR-24h is shown in the heatmap (left). Differential expression of the miRNAs after screening based on *P* values ($P < 0.05$) between Exo-Normal and Exo-IR-24h is shown in the heatmap (right). All experiments were performed in triplicate, $n = 12$ mice/group.

To further validate the effect of exosomes on IR-induced intestinal injury, we performed functional experiments in vitro using MODE-K murine intestinal epithelial cells. As expected, treatment with Exo-IR-24h enhanced the suppression of IR-induced cell proliferation, whereas Exo-Normal had no significant effect on the cells. Moreover, treatment with Exo-IR-24h increased ROS production and the level of phosphorylated H2AX in irradiated MODE-K cells, which was consistent with our previous in vivo results. Nuclear factor erythroid 2-related factor 2 (Nrf2) is a nuclear transcription factor that mediates the primary cellular

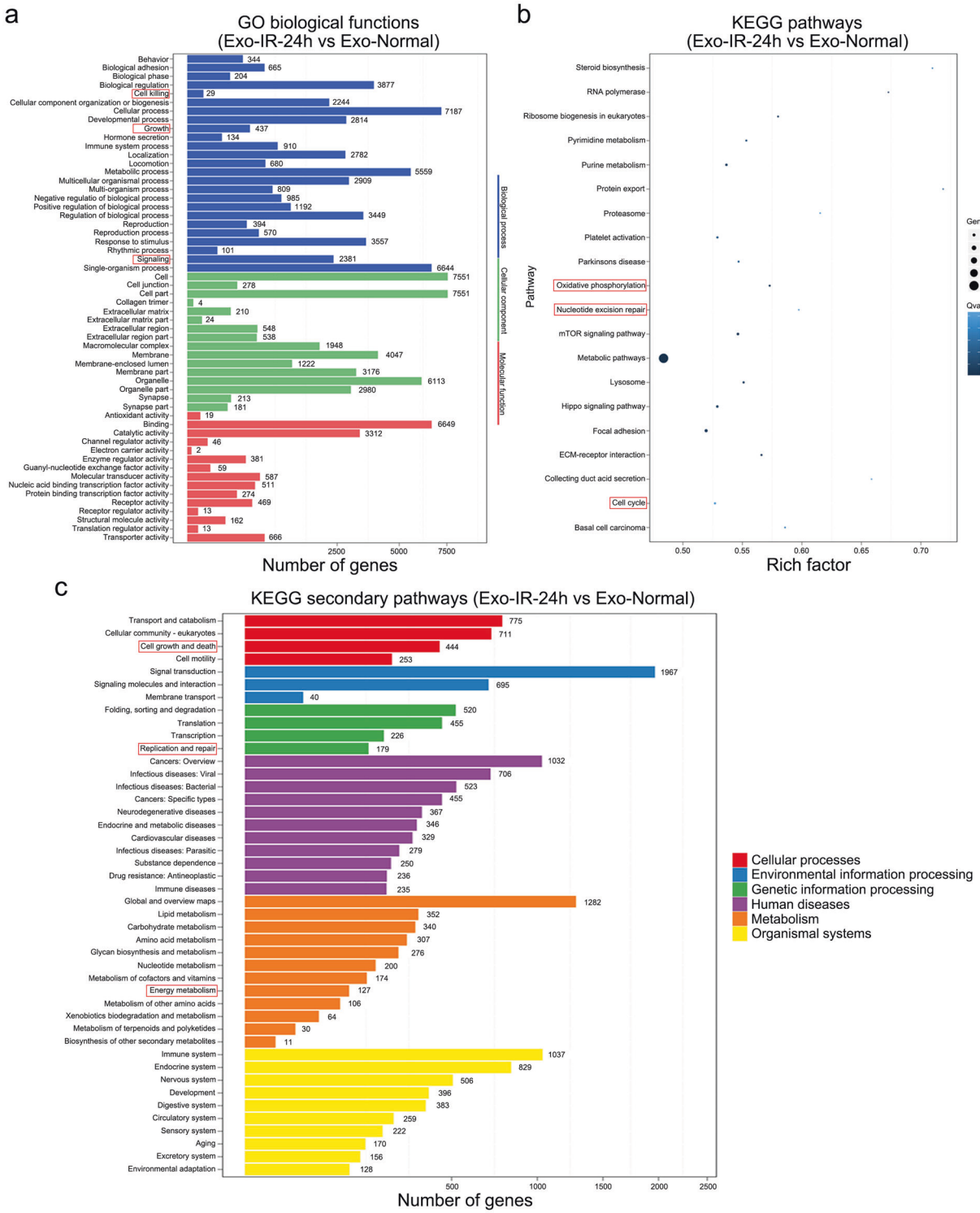

Fig. 8 The GO biological processes and KEGG pathways significantly enriched with putative genes targeted by the exosomal microRNAs. **a** GO biological processes. **b** KEGG pathways. **c** Secondary KEGG pathways.

defense against the cytotoxic effects of oxidative stress [59]. Previous research revealed that activation of Nrf2 can induce a self-protective antioxidant defense program, reducing DNA damage after irradiation [60, 61]. Herein, our data demonstrated that treatment with Exo-IR-24h downregulated the expression of Nrf2 and its targets (HO-1 and NQO1), interfering with the antioxidant response in intestinal cells after IR. Collectively, these results indicated that treatment with Exo-IR-24h further suppressed cell proliferation and promoted oxidative DNA damage after IR in vitro.

Exosomes improve communication among cells or tissues by transferring numerous different functional molecules, such as DNAs, mRNAs, proteins and especially miRNAs, to recipient cells [62]. It has been shown that miRNAs can regulate a variety of biological processes in the injured small intestine of mice after high-dose radiation exposure [6]. In this study, we identified thousands of

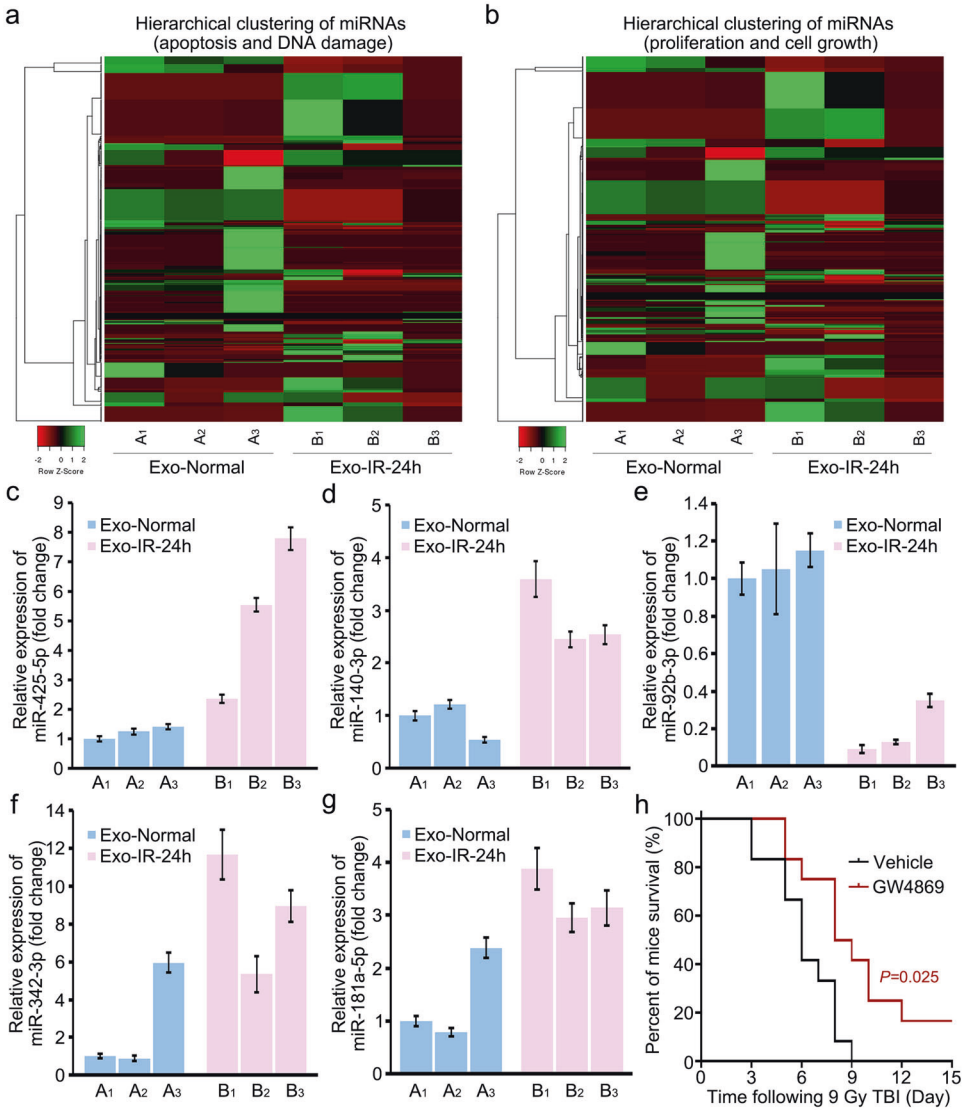

Fig. 9 Total body irradiation induces intestinal injury through serum exosomal miRNAs in mice. a Differential expression of apoptosis- and DNA damage-related miRNAs between Exo-Normal and Exo-IR-24h is shown in the heatmap. **b** Differential expression of proliferation- and cell growth-related miRNAs between Exo-Normal and Exo-IR-24h is shown in the heatmap. **c–g** The expression levels of 5 miRNAs randomly selected from those listed in (**a**) and (**b**) were determined by real-time PCR in the intestinal tissues of mice treated with Exo-Normal or Exo-IR-24h after TBI. **h** Kaplan–Meier survival analysis of mice treated or not treated with GW4869 (an inhibitor of exosome biogenesis and release) after 9 Gy TBI (n=12 mice/group).

miRNAs that could be modulated by TBI in the exosomes of mice. To further explore the functions of these exosomal miRNAs, we sought to identify the predicted target genes of these miRNAs and analyzed their GO annotations and related pathways by using bioinformatics tools. We found that these miRNAs regulated a large number of genes in several key signaling pathways, including pathways related to oxidative phosphorylation, nucleotide excision repair, the cell cycle, DNA replication and repair, cell growth and death, and energy metabolism. A previous report suggested that specific biological processes, including apoptosis, DNA damage, proliferation and cell growth, are the main contributors to IR-induced intestinal damage [63–65]. Therefore, we performed heatmap analysis with the exosomal miRNAs that were involved in the abovementioned processes. In summary, our data showed that TBI induces intestinal injury through serum exosomal miRNAs in mice.

The components of blood or serum in animals can be regulated after irradiation in a time-dependent manner [66–68]. Hence, we assumed that the cargo of exosomes secreted from cells could be altered at different times after irradiation in mice. As expected, our results confirmed that exosomes isolated from the serum of mice after 24 h of TBI had a significant promotive effect on IR-induced intestinal damage, suggesting that TBI induces intestinal injury through exosomes secreted in vivo. Accordingly, we further proved that inhibition of exosome biogenesis after 24 h of TBI protects mice against TBI-induced lethality and intestinal damage. In addition, we found that Exo-IR-24h had no effect on the survival rate of mice exposed to a nonlethal dose of TBI (Supplementary Fig. S5), indicating that the exosomes secreted in vivo only act as vehicles during TBI-induced intestinal damage or death in mice.

In summary, our study illustrates the mechanism by which TBI induces intestinal injury through exosomes in vivo (Fig. 10), providing a new therapeutic strategy to combat clinical intestinal damage caused by ionizing radiation.

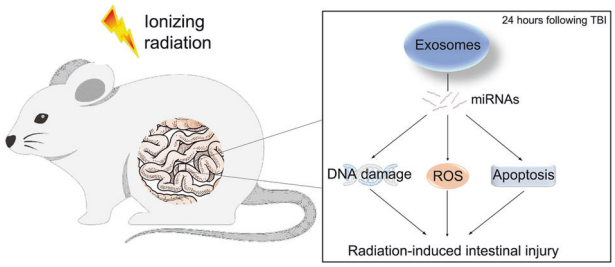

Fig. 10 Exosomes are involved in total body irradiation-induced intestinal injury in mice. Total body irradiation induces intestinal injury in mice through miRNAs contained in exosomes secreted in vivo after 24 h of TBI.

ACKNOWLEDGEMENTS

This work was supported by grants from the National Natural Science Foundation of China (No. 81803046 and No. 81730086), the Natural Science Foundation of Tianjin City (19JCQNJC09700), and the CAMS Innovation Fund for Medical Sciences (2017-I2M-B&R-13).

AUTHOR CONTRIBUTIONS

HL and SJF conceived the project idea and designed the experiments. HL, MJ, SYZ and SQZ performed the experiments. LL and GXF performed data analysis. XH and XW assisted in data interpretation and manuscript revision. HL drafted the article and wrote the entire manuscript. All authors commented on and approved the manuscript.

ADDITIONAL INFORMATION

Supplementary information The online version contains supplementary material available at https://doi.org/10.1038/s41401-021-00615-6.

Competing interests: The authors declare no competing interests.

REFERENCES

1. Dutta A, Gupta ML, Verma S. Podophyllotoxin and rutin in combination prevents oxidative stress mediated cell death and advances revival of mice gastrointestine following lethal radiation injury. Free Radic Res. 2018;52:103–17.
2. Carter CL, Hankey KG, Booth C, Tudor GL, Parker GA, Jones JW, et al. Characterizing the natural history of acute radiation syndrome of the gastrointestinal tract: combining high mass and spatial resolution using maldi-fticr-msi. Health Phys. 2019;116:454–72.
3. MacVittie TJ, Farese AM, Parker GA, Jackson W 3rd, Booth C, Tudor GL, et al. The gastrointestinal subsyndrome of the acute radiation syndrome in rhesus macaques: a systematic review of the lethal dose-response relationship with and without medical management. Health Phys. 2019;116:305–38.
4. Cao J, Li H, Yuan R, Dong Y, Wu J, Wang M, et al. Protective effects of new aryl sulfone derivatives against radiation-induced hematopoietic injury. J Radiat Res. 2020;61:388–98.
5. Xu G, Wu H, Zhang J, Li D, Wang Y, Wang Y, et al. Metformin ameliorates ionizing irradiation-induced long-term hematopoietic stem cell injury in mice. Free Radic Biol Med. 2015;87:15–25.
6. Chiba M, Uehara H, Niiyama I, Kuwata H, Monzen S. Changes in mirna expressions in the injured small intestine of mice following highdose radiation exposure. Mol Med Rep. 2020;21:2452–8.
7. Dong Y, Cheng Y, Hou Q, Wu J, Li D, Tian H. The protective effect of new compound xh-103 on radiation-induced gi syndrome. Oxid Med Cell Longev. 2018;2018:3920147.
8. Holler V, Buard V, Roque T, Squiban C, Benderitter M, Flamant S, et al. Early and late protective effect of bone marrow mononuclear cell transplantation on radiation-induced vascular dysfunction and skin lesions. Cell Transpl. 2019;28:116–28.
9. Lu L, Jiang M, Zhu C, He J, Fan S. Amelioration of whole abdominal irradiation-induced intestinal injury in mice with 3,3′-diindolylmethane (dim). Free Radic Biol Med. 2019;130:244–55.
10. Jabbour SK, Patel S, Herman JM, Wild A, Nagda SN, Altoos T, et al. Intensity-modulated radiation therapy for rectal carcinoma can reduce treatment breaks and emergency department visits. Int J Surg Oncol. 2012;2012:891067.
11. Mashouri L, Yousefi H, Aref AR, Ahadi AM, Molaei F, Alahari SK. Exosomes: Composition, biogenesis, and mechanisms in cancer metastasis and drug resistance. Mol Cancer. 2019;18:75.
12. Su X, Shen Y, Jin Y, Weintraub NL, Tang YL. Identification of critical molecular pathways involved in exosome-mediated improvement of cardiac function in a mouse model of muscular dystrophy. Acta Pharmacol Sin. 2020. https://doi.org/10.1038/s41401-020-0446-y.
13. Fang T, Lv H, Lv G, Li T, Wang C, Han Q, et al. Tumor-derived exosomal mir-1247-3p induces cancer-associated fibroblast activation to foster lung metastasis of liver cancer. Nat Commun. 2018;9:191.
14. Murdica V, Giacomini E, Makieva S, Zarovni N, Candiani M, Salonia A, et al. In vitro cultured human endometrial cells release extracellular vesicles that can be uptaken by spermatozoa. Sci Rep. 2020;10:8856.
15. Sun XH, Wang YT, Li GF, Zhang N, Fan L. Serum-derived three-circrna signature as a diagnostic biomarker for hepatocellular carcinoma. Cancer Cell Int. 2020;20:226.
16. Zhou X, Xie F, Wang L, Zhang L, Zhang S, Fang M, et al. The function and clinical application of extracellular vesicles in innate immune regulation. Cell Mol Immunol. 2020;17:323–34.
17. Rao Q, Zuo B, Lu Z, Gao X, You A, Wu C, et al. Tumor-derived exosomes elicit tumor suppression in murine hepatocellular carcinoma models and humans in vitro. Hepatology. 2016;64:456–72.
18. Li SP, Lin ZX, Jiang XY, Yu XY. Exosomal cargo-loading and synthetic exosome-mimics as potential therapeutic tools. Acta Pharmacol Sin. 2018;39:542–51.
19. Jacques C, Tesfaye R, Lavaud M, Georges S, Baud'huin M, Lamoureux F, et al. Implication of the p53-related mir-34c, -125b, and -203 in the osteoblastic differentiation and the malignant transformation of bone sarcomas. Cells. 2020;9:810.
20. Endzelins E, Berger A, Melne V, Bajo-Santos C, Sobolevska K, Abols A, et al. Detection of circulating mirnas: Comparative analysis of extracellular vesicle-incorporated mirnas and cell-free mirnas in whole plasma of prostate cancer patients. BMC Cancer. 2017;17:730.
21. Malla B, Aebersold DM, Dal, Pra A. Protocol for serum exosomal mirnas analysis in prostate cancer patients treated with radiotherapy. J Transl Med. 2018;16:223.
22. Ferrao ML, Rocha MJ, Rocha E. Histological characterization of the maturation stages of the ovarian follicles of the goldfish carassius auratus (linnaeus, 1758). Anat Histol Embryol. 2020;49:749–62.
23. Wei S, Cheng F, Yu W. Pathological analysis on transurethral enucleation resection of the prostate-related prostate surgical capsule. Wideochir Inne Tech Maloinwazyjne. 2019;14:255–61.
24. Martin ML, Adileh M, Hsu KS, Hua G, Lee SG, Li C, et al. Organoids reveal that inherent radiosensitivity of small and large intestinal stem cells determines organ sensitivity. Cancer Res. 2020;80:1219–27.
25. Lee C, Choi C, Kang HS, Shin SW, Kim SY, Park HC, et al. Nod2 supports crypt survival and epithelial regeneration after radiation-induced injury. Int J Mol Sci. 2019;20:4297.
26. Ling Y, Suying F, Zhiliang L, Peiying J, Baoxi W, Lin L. Application of indirect immunofluorescence on the diagnosis of pemphigus. Acta Dermatovenerol Croat. 2019;27:142–5.
27. Russell JO, Lu WY, Okabe H, Abrams M, Oertel M, Poddar M, et al. Hepatocyte-specific beta-catenin deletion during severe liver injury provokes cholangiocytes to differentiate into hepatocytes. Hepatology. 2019;69:742–59.
28. Kumar P, Nagarajan A, Uchil PD. Analysis of cell viability by the mtt assay. Cold Spring Harb Protoc. 2018;2018. https://doi.org/10.1101/pdb.prot095505.
29. Graziani F, Pinton P, Olleik H, Pujol A, Nicoletti C, Sicre M, et al. Deoxynivalenol inhibits the expression of trefoil factors (tff) by intestinal human and porcine goblet cells. Arch Toxicol. 2019;93:1039–49.
30. Levy A, Stedman A, Deutsch E, Donnadieu F, Virgin HW, Sansonetti PJ, et al. Innate immune receptor nod2 mediates lgr5(+) intestinal stem cell protection against ros cytotoxicity via mitophagy stimulation. Proc Natl Acad Sci USA. 2020;117:1994–2003.
31. Metcalfe C, Kljavin NM, Ybarra R, de Sauvage FJ. Lgr5^{+} stem cells are indispensable for radiation-induced intestinal regeneration. Cell Stem Cell. 2014;14:149–59.
32. Basak O, Beumer J, Wiebrands K, Seno H, van Oudenaarden A, Clevers H. Induced quiescence of lgr5^{+} stem cells in intestinal organoids enables differentiation of hormone-producing enteroendocrine cells. Cell Stem Cell. 2017;20:177–90.e4.
33. Takakuwa A, Nakamura K, Kikuchi M, Sugimoto R, Ohira S, Yokoi Y, et al. Butyric acid and leucine induce alpha-defensin secretion from small intestinal paneth cells. Nutrients. 2019;11:2817. https://doi.org/10.3390/nu11112817.
34. Cheung R, Kelly J, Macleod RJ. Regulation of villin by wnt5a/ror2 signaling in human intestinal cells. Front Physiol. 2011;2:58.
35. Khan K, Tewari S, Awasthi NP, Mishra SP, Agarwal GR, Rastogi M, et al. Flow cytometric detection of gamma-h2ax to evaluate DNA damage by low dose diagnostic irradiation. Med Hypotheses. 2018;115:22–28.

36. Liu Q, Si T, Xu X, Liang F, Wang L, Pan S. Electromagnetic radiation at 900 mhz induces sperm apoptosis through bcl-2, bax and caspase-3 signaling pathways in rats. Reprod Health. 2015;12:65.
37. Mizuta Y, Tokuda K, Guo J, Zhang S, Narahara S, Kawano T, et al. Sodium thiosulfate prevents doxorubicin-induced DNA damage and apoptosis in cardiomyocytes in mice. Life Sci. 2020;257:118074.
38. Wang L, Wulf GM. Not black or white but shades of gray: Homologous recombination deficiency as a continuous variable modulated by rnf168. Cancer Res. 2020;80:2720–1.
39. Zhu HF, Yan PW, Wang LJ, Liu YT, Wen J, Zhang Q, et al. Protective properties of huperzine a through activation nrf2/are-mediated transcriptional response in x-rays radiation-induced nih3t3 cells. J Cell Biochem. 2018;119:8359–67.
40. Zhou YQ, Liu DQ, Chen SP, Chen N, Sun J, Wang XM, et al. Nrf2 activation ameliorates mechanical allodynia in paclitaxel-induced neuropathic pain. Acta Pharmacol Sin. 2020;41:1041–8.
41. Zhu B, Zhang L, Liang C, Liu B, Pan X, Wang Y, et al. Stem cell-derived exosomes prevent aging-induced cardiac dysfunction through a novel exosome/lncrna malat1/nf-kappab/tnf-alpha signaling pathway. Oxid Med Cell Longev. 2019;2019:9739258.
42. Wang Y, Jia L, Xie Y, Cai Z, Liu Z, Shen J, et al. Involvement of macrophage-derived exosomes in abdominal aortic aneurysms development. Atherosclerosis. 2019;289:64–72.
43. Bhanja P, Saha S, Kabarriti R, Liu L, Roy-Chowdhury N, Roy-Chowdhury J, et al. Protective role of r-spondin1, an intestinal stem cell growth factor, against radiation-induced gastrointestinal syndrome in mice. PLoS ONE. 2009;4:e8014.
44. Kong F, Wu CT, Geng P, Liu C, Xiao F, Wang LS, et al. Dental pulp stem cell-derived extracellular vesicles mitigate haematopoietic damage after radiation. Stem Cell Rev Rep. 2020. https://doi.org/10.1007/s12015-020-10020-x.
45. Chou DB, Frismantas V, Milton Y, David R, Pop-Damkov P, Ferguson D, et al. On-chip recapitulation of clinical bone marrow toxicities and patient-specific pathophysiology. Nat Biomed Eng. 2020;4:394–406.
46. Zhao Z, Qu W, Wang K, Chen S, Zhang L, Wu D, et al. Bisphenol a inhibits mucin 2 secretion in intestinal goblet cells through mitochondrial dysfunction and oxidative stress. Biomed Pharmacother. 2019;111:901–8.
47. Venkateswaran K, Shrivastava A, Agrawala PK, Prasad AK, Devi SC, Manda K, et al. Mitigation of radiation-induced gastro-intestinal injury by the polyphenolic acetate 7, 8-diacetoxy-4-methylthiocoumarin in mice. Sci Rep. 2019;9:14134.
48. Li Q, Sun Y, Jarugumilli GK, Liu S, Dang K, Cotton JL, et al. Lats1/2 sustain intestinal stem cells and wnt activation through tead-dependent and independent transcription. Cell Stem Cell. 2020;26:675–92.e8.
49. Mundorf J, Donohoe CD, McClure CD, Southall TD, Uhlirova M. Ets21c governs tissue renewal, stress tolerance, and aging in the drosophila intestine. Cell Rep. 2019;27:3019–33.e5.
50. Setiawan J, Kotani T, Konno T, Saito Y, Murata Y, Noda T, et al. Regulation of small intestinal epithelial homeostasis by tsc2-mtorc1 signaling. Kobe J Med Sci. 2019;64:E200–E209.
51. Etemadi T, Momeni HR, Ghafarizadeh AA. Impact of silymarin on cadmium-induced apoptosis in human spermatozoa. Andrologia. 2020;52:e13795.
52. Zhu N, Liu R, He LX, Mao RX, Liu XR, Zhang T, et al. Radioprotective effect of walnut oligopeptides against gamma radiation-induced splenocyte apoptosis and intestinal injury in mice. Molecules. 2019;24:1582.
53. Liu Z, Liu H, Jiang J, Tan S, Yang Y, Zhan Y, et al. Pdgf-bb and bfgf ameliorate radiation-induced intestinal progenitor/stem cell apoptosis via akt/p53 signaling in mice. Am J Physiol Gastrointest Liver Physiol. 2014;307:G1033–43.
54. Ai TJ, Sun JY, Du LJ, Shi C, Li C, Sun XN, et al. Inhibition of neddylation by mln4924 improves neointimal hyperplasia and promotes apoptosis of vascular smooth muscle cells through p53 and p62. Cell Death Differ. 2018;25:319–29.
55. Yu G, Luo H, Zhang N, Wang Y, Li Y, Huang H, et al. Loss of p53 sensitizes cells to palmitic acid-induced apoptosis by reactive oxygen species accumulation. Int J Mol Sci. 2019;20:6268.
56. Penha RCC, Pellecchia S, Pacelli R, Pinto LFR, Fusco A. Ionizing radiation deregulates the microrna expression profile in differentiated thyroid cells. Thyroid. 2018;28:407–21.
57. Xiao AY, Maynard MR, Piett CG, Nagel ZD, Alexander JS, Kevil CG, et al. Sodium sulfide selectively induces oxidative stress, DNA damage, and mitochondrial dysfunction and radiosensitizes glioblastoma (gbm) cells. Redox Biol. 2019;26:101220.
58. Sharma D, De Falco L, Padavattan S, Rao C, Geifman-Shochat S, Liu CF, et al. Parp1 exhibits enhanced association and catalytic efficiency with gammah2a.X-nucleosome. Nat Commun. 2019;10:5751.
59. Lu M, Wang P, Qiao Y, Jiang C, Ge Y, Flickinger B, et al. Gsk3beta-mediated keap1-independent regulation of Nrf2 antioxidant response: a molecular rheostat of acute kidney injury to chronic kidney disease transition. Redox Biol. 2019;26:101275.
60. Resendez A, Tailor D, Graves E, Malhotra SV. Radiosensitization of head and neck squamous cell carcinoma (HNSCC) by a podophyllotoxin. ACS Med Chem Lett. 2019;10:1314–21.
61. Chaiprasongsuk A, Janjetovic Z, Kim TK, Jarrett SG, D'Orazio JA, Holick MF, et al. Protective effects of novel derivatives of vitamin d3 and lumisterol against uvb-induced damage in human keratinocytes involve activation of Nrf2 and p53 defense mechanisms. Redox Biol. 2019;24:101206.
62. Zhou Q, Huang SX, Zhang F, Li SJ, Liu C, Xi YY, et al. Micrornas: A novel potential biomarker for diagnosis and therapy in patients with non-small cell lung cancer. Cell Prolif. 2017;50:e12394.
63. Wang W, Hu L, Chang S, Ma L, Li X, Yang Z, et al. Total body irradiation-induced colon damage is prevented by nitrate-mediated suppression of oxidative stress and homeostasis of the gut microbiome. Nitric Oxide. 2020;102:1–11.
64. Li L, Zhang K, Zhang J, Zeng YN, Lai F, Li G, et al. Protective effect of polydatin on radiation-induced injury of intestinal epithelial and endothelial cells. Biosci Rep. 2018;38:BSR20180868.
65. Verginadis II, Kanade R, Bell B, Koduri S, Ben-Josef E, Koumenis C. A novel mouse model to study image-guided, radiation-induced intestinal injury and preclinical screening of radioprotectors. Cancer Res. 2017;77:908–17.
66. Lewicka M, Henrykowska G, Zawadzka M, Rutkowski M, Pacholski K, Buczynski A. Impact of electromagnetic radiation emitted by monitors on changes in the cellular membrane structure and protective antioxidant effect of vitamin A–in vitro study. Int J Occup Med Environ Health. 2017;30:695–703.
67. Zhang J, Han X, Zhao Y, Xue X, Fan S. Mouse serum protects against total body irradiation-induced hematopoietic system injury by improving the systemic environment after radiation. Free Radic Biol Med. 2019;131:382–92.
68. Tai S, Yang S, Tiew A, Wong YM, Ling SY, Tay YS, et al. Radiation exposure to allied health personnel handling blood specimens from patients receiving radioactive iodine-131 and recombinant human TSH (Thyrogen®) stimulation. J Radiol Prot. 2020. https://iopscience.iop.org/article/10.1088/1361-6498/ab9507.